

14. Le Barney, P., Bouche, C. M., Facchetti, H., Soyer, F. & Robin, P. Synthesis of side chain electroluminescent polymers and properties of devices including them. *Proc. SPIE* **3148**, 160–169 (1997).
15. Bellmann, E. *et al.* New triarylamine-containing polymers as hole transport materials in organic light-emitting diodes: effect of polymer structure and crosslinking on device characteristics. *Chem. Mater.* **10**, 1668–1676 (1998).
16. Jiang, X., Liu, S., Ma, H. & Jen, A. K. High-performance blue light-emitting diode based on a binaphthyl-containing polyfluorene. *Appl. Phys. Lett.* **76**, 1813–1815 (2000).
17. Bacher, A. *et al.* Photo-cross-linked triphenylenes as novel insoluble hole transport materials in organic LEDs. *Macromolecules* **32**, 4551–4557 (1999).
18. Li, W. *et al.* Covalently interlinked organic LED transport layers via spin-coating/siloxane condensation. *Adv. Mater.* **11**, 730–734 (1999).
19. Chen, J. P. *et al.* Efficient, blue light-emitting diodes using cross-linked layers of polymeric arylamine and fluorene. *Synth. Met.* **107**, 129–135 (1999).
20. Becker, H., Heun, S., Treacher, K., Büsing, A. & Falcou, A. Materials and inks for full-colour PLED displays. *SID Digest Tech. Pap.* **33**, 780–782 (2002).
21. Fouassier, J.-P. *Photoinitiation, Photopolymerization, and Photocuring: Fundamentals and Applications* 102–144 (Hanser/Gardner, Cincinnati, 1995).
22. Sasaki, H. & Crivello, J. V. The synthesis, characterization, and photoinitiated cationic polymerization of difunctional oxetanes. *J. Macromol. Sci. A* **29**, 915–930 (1992).
23. Penczek, S. & Kubisa, P. in *Comprehensive Polymer Science* (ed. Allen, G.) Vol. III, 751–786 (Pergamon, Oxford, 1989).
24. Treacher, K. *et al.* Conjugated polymers containing spirofluorene units and fluorene units, and the use thereof. German patent application DE 2001-10114477; WO 2002-077060.

Acknowledgements Partial financial support was granted by the Deutsche Forschungsgemeinschaft, the Bundesministerium für Bildung und Forschung, the Fonds der Chemischen Industrie (Kekule grant for N.R.), and the Bavarian government through 'Neue Werkstoffe'.

Competing interests statement The authors declare that they have no competing financial interests.

Correspondence and requests for materials should be addressed to K.M. (e-mail: klaus.meerholz@uni-koeln.de).

Precise dating of Dansgaard–Oeschger climate oscillations in western Europe from stalagmite data

D. Genty*, D. Blamart*, R. Ouahdi*, M. Gilmour†, A. Baker‡, J. Jouzel* & Sandra Van-Exter§

* IPSL/Laboratoire des Sciences du Climat et de l'Environnement, UMR CEA/CNRS 1572 Bat. 709, L'Orme des Merisiers CEA Saclay, 91191 Gif sur Yvette cedex, France

† The Open University, Department of Earth Sciences, Uranium Series Facility, Milton Keynes MK7 6AA, UK

‡ Centre for Land Use and Water Resources Research, University of Newcastle upon Tyne, Newcastle upon Tyne NE1 7RU, UK

§ University of Montpellier, Laboratoire Hydrosociences, UMR 5569 (CNRS-UM2-IRD), Maison des sciences de l'eau, CC 057, Place E. Bataillon, 34095 Montpellier cedex 5, France

The signature of Dansgaard–Oeschger events—millennial-scale abrupt climate oscillations during the last glacial period—is well established in ice cores and marine records^{1–3}. But the effects of such events in continental settings are not as clear, and their absolute chronology is uncertain beyond the limit of ¹⁴C dating and annual layer counting for marine records and ice cores, respectively. Here we present carbon and oxygen isotope records from a stalagmite collected in southwest France which have been precisely dated using ²³⁴U/²³⁰Th ratios. We find rapid climate oscillations coincident with the established Dansgaard–Oeschger events between 83,000 and 32,000 years ago in both isotope records. The oxygen isotope signature is similar to a record from Soreq cave, Israel⁴, and deep-sea records^{5,6}, indicating the large spatial scale of the climate oscillations. The signal in the carbon isotopes gives evidence of drastic and rapid vegetation

changes in western Europe, an important site in human cultural evolution. We also find evidence for a long phase of extremely cold climate in southwest France between 61.2 ± 0.6 and 67.4 ± 0.9 kyr ago.

Several of the 24 Dansgaard–Oeschger (DO) events identified in the GRIP^{7,8} and GISP2⁹ Greenland ice cores over the last glacial period indicate air temperature changes greater than 10 °C. North Atlantic and Mediterranean marine cores show similar amplitude changes in the water temperature^{5,10,11}. However, the consequences of these events on the continent are still not well known, because of the scarcity of well-preserved and well-dated records. We know that the ocean–atmosphere system was closely coupled as far as the central Mediterranean region, where the vegetation has been reconstructed thanks to pollen records (in lakes) that reacted very quickly and sensitively to these abrupt climate changes^{12,13}. GRIP and GISP2 dating uncertainties may exceed the duration of a single DO event for a large part of the glacial period (estimated for GISP2 at 2% over the past 40 kyr, and between 5% and 10% for the period <50 kyr ago^{14,15}). Marine cores are dated by orbital tuning with inherent accuracy and, for their late-glacial part, by ¹⁴C dating. However, for periods of interest here, this latter method suffers from limitations linked with analytical precision, ¹⁴C age calibration, fluctuations in the carbon cycle, and a varying age reservoir¹⁶. The few continental records also display a lack of absolute ages, especially after 40 kyr ago^{12,13}. This highlights the importance of establishing chronologies of those events from other records.

Here we present stable isotope records ($\delta^{13}\text{C}$ and $\delta^{18}\text{O}$) from a stalagmite of the Villars cave (southwest France, less than 200 km from the Atlantic Ocean; Fig. 1) that show most of the DO events between 83 and 32 kyr ago (Fig. 2). We have determined 27 thermal ionization mass spectrometry (TIMS) U-series dates on this 147-cm-long stalagmite ('Vil9'), leading to an absolute timescale with errors less than 2% (2σ) up to 83 kyr ago (see Supplementary Table 1 for information, and ref. 17 for methods). Three main hiatuses occurred at 78.8–75.5 kyr ago (referred to as D2), 67.4–61.2 kyr ago (D3) and 55.7–51.8 kyr ago (D4). The regular $\delta^{13}\text{C}$ and $\delta^{18}\text{O}$ decreases towards the D3 hiatus, and also the steady increase that is observed afterwards, suggests that this growth cessation is

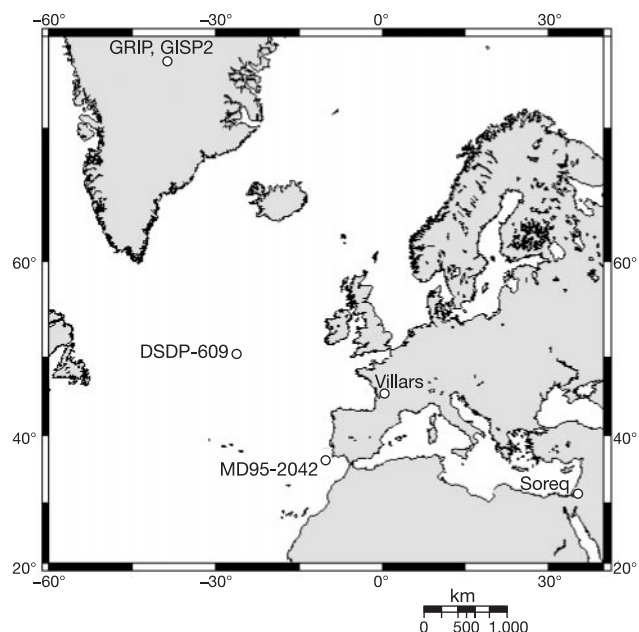


Figure 1 Map showing locations of the study sites. GRIP and GISP2; 72.58° N, 37.64° W. Villars cave; 45.30° N, 0.50° E. MD95-2042; 37.48° N, 10.10° W. DSDP 609; 50° N, 27° W. Soreq cave; 31.6° N, 35° E.

related to climatic and/or vegetation causes. The timing of D3 is in good temporal agreement with Heinrich event H6, whose duration, from other records, is not well constrained⁵. This confirms that the climate switched to much colder conditions leading to the cessation of stalagmite growth for about 6.2 kyr, which is one of the main features of the Vil9 record ('Villars cold phase', Fig. 3). Because D2 and D4 hiatuses occurred during stable or low $\delta^{13}\text{C}$ and $\delta^{18}\text{O}$ levels, their cause is possibly different from that of D3 (perhaps flooding). The other visible discontinuities, where no growth hiatus occurred, are due either to very short cessations, or to short events that

brought detrital particles onto the stalagmite growth surface (such as flooding or micro-fissure emptying). The fact that the other Heinrich events (that is, H4, H5) are not recorded on our sample as growth cessations suggests that they led to less-drastring climatic conditions in southwest France, as is also suggested by nearby marine cores DSDP-609 and MD95-2042 (Figs 3 and 4).

DO events are particularly visible in the carbon isotope record, with typically 2–4‰ variations in the $\delta^{13}\text{C}$. A comparison with $\delta^{18}\text{O}$ GRIP and GISP2 records allows their identification, low $\delta^{13}\text{C}$ values corresponding to high ice $\delta^{18}\text{O}$ and thus to warmer conditions and,

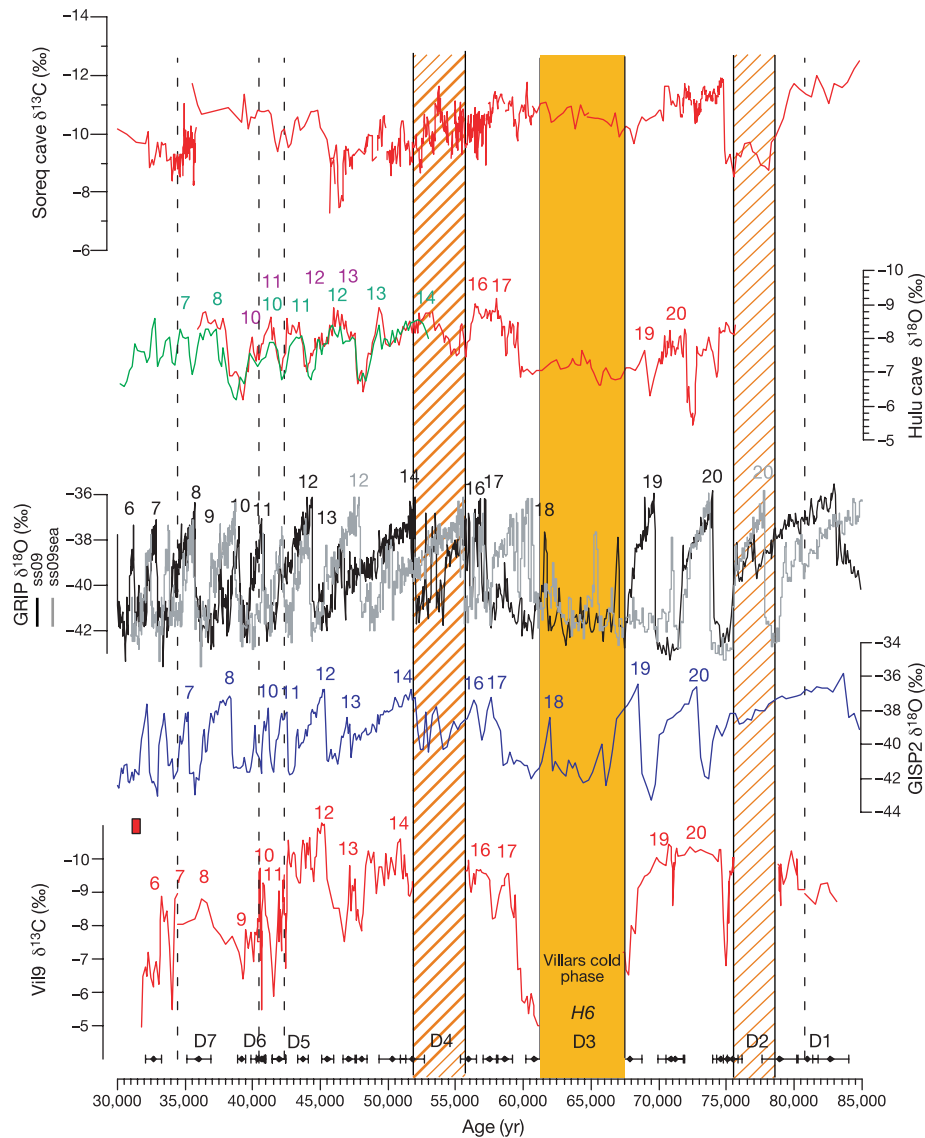


Figure 2 Comparison of the Vil9 stalagmite carbon isotope profile with Greenland ice core records and other stalagmite records. Vil9 stalagmite $\delta^{13}\text{C}$ record compared with GISP2 ice core $\delta^{18}\text{O}$ (ref. 9), GRIP ice core $\delta^{18}\text{O}$ (ss09 chronology; ref. 8), GRIP ice core $\delta^{18}\text{O}$ (ss09sea chronology; ref. 24). Note that DO events from GRIP ss09sea chronology are all significantly older than in Vil9 DO with a lag of about one entire event. Also shown are records from Hulu cave (China) stalagmite $\delta^{18}\text{O}$ (ref. 18) and from Soreq cave, Israel ($\delta^{13}\text{C}$) (ref. 4). The fact that the Soreq cave $\delta^{13}\text{C}$ record does not show the same features can be explained either by difference in local hydrology and by local vegetation influences (that is, C_4 type) or because it is too far from the Atlantic. At the bottom of the figure, D1–D7 indicate visible discontinuities, and H6 shows a Heinrich event. Modern calcite $\delta^{13}\text{C}$ values at Villars correspond to the red rectangle at the bottom left. Our chronology, like all others that use absolute U-series ages, might have been affected by an ‘accordion’

effect because growth rate is likely to have changed with climate: growth rate is 0.1 mm yr^{-1} during DO 12, one of the warmest events, whereas it is 0.01 mm yr^{-1} at the end of the stalagmite growth, the coldest period which led to the definitive stop of the growth. Speleothem growth rate is mainly controlled by the seepage water calcium concentration and by the drip rate²⁵. In the studied area, and for the present day, it varies from 0.3 mm yr^{-1} to about 1.0 mm yr^{-1} (ref. 26). It is likely that during cold periods, the calcium concentration in the seepage water was lower, owing to lower vegetation activity, leading to a slower growth rate. This might have happened between each warm phase of DO events; however, we have dated points that surround these cold phases (between DO 19 and 20, before DO 20, between DO 10 and 11), and it appears that their durations are not particularly long (that is, less than 1 kyr). Coloured vertical bars represent growth hiatuses.

at least in Greenland, to higher precipitation (Fig. 2). Most of GISP2 DO ages are within the 2σ error limits, except for DO 8, 19 and 20. DO 8 displays a regular $\delta^{13}\text{C}$ decrease from 39.4 to 36.2 kyr ago whose shape is very similar to the Hulu cave record¹⁸. DO 19 and 20 events are significantly older in our record, and are better correlated with the GRIP (ss09) record. The duration of the cold phases surrounding these two former events seems to have been very short, as shown by the four U/Th ages that have been determined just at the edge of their limits (Fig. 2). DO 12 reached its optimum (lower $\delta^{13}\text{C}$) at 45.3 ± 0.4 kyr ago, similar to the GISP2 chronology and about 1,000 yr older than in GRIP ss09 chronology, but it seems to have started much earlier at about 46.8 ± 0.4 kyr ago. DO 12 is also the most pronounced event, as determined by its stable isotope amplitude variation, by its duration and by the stalagmite growth rate: between 42.3 and 45.5 kyr ago, 16% of the Vil9 height grew for less than 6% of its growth duration. DO 12 is characterized by a well-marked saw-tooth shape, very similar to the GRIP record with a $\delta^{13}\text{C}$ decrease (climate amelioration) that is clearly visible at the end of the event, just before its abrupt termination at 42.3 kyr ago (Fig. 2). DO events 6 to 14 have been enumerated by reference to DO 12, but we note that their chronology is less clear between DO 8 and 12. The Hulu cave record¹⁸ agrees well with our results if we consider the second chronology (Hulu cave 2), but DO 12 still seems too young (by 1.5 kyr) or too old (by 2.2 kyr) depending on the adopted chronology. We note also that DO 19 is much more pronounced in the Vil9 record.

Considering that most of the record was deposited under isotopic equilibrium (Supplementary Information), the fact that the DO events are so clearly recorded in the $\delta^{13}\text{C}$ profile may be explained as follows. First, a change in the ratio of C_4 plants to C_3 plants suggested in other studies¹⁹ cannot be invoked here, as, until now,

no evidence of C_4 plants have been found in this area during the last glacial. Second, we have shown that most of the carbon (80–90%) of the stalagmites, at least in Villars, comes from the soil CO_2 , and that any change in biologic soil activity conditions will change the carbon isotope signature of these stalagmites¹⁷. Consequently, degradation of vegetation and soil will decrease the biogenic CO_2 production and increase the relative proportion of atmospheric CO_2 , establishing a direct link with temperature and precipitation changes associated with DO events. Two observations support this interpretation: first the $\delta^{13}\text{C}$ of present-day calcite is much higher in caves above which the soil is poor²⁰; second, $\delta^{13}\text{C}$ records of the last glacial–interglacial transition in a stalagmite from southern France show much higher $\delta^{13}\text{C}$ values (that is, $>5\text{‰}$) during the late glacial than during the Holocene (D.G. *et al.*, unpublished results).

Here we suggest that temperature and humidity were important in the development of local vegetation, and consequently in the production of soil CO_2 : Vil9 $\delta^{13}\text{C}$ is lower during warm periods because a higher proportion of biogenic CO_2 is dissolved in the seepage water. Clear similarities with the MD-95-2042 $\delta^{18}\text{O}$ planktonic record⁶ and with the DSDP-609 foraminifera record⁵, both close to the Villars cave (Fig. 1), support this interpretation (Fig. 3). The time lag between the climate amelioration and the vegetation change seems to have been relatively short for most of the observed DO events, as suggested by the rapid $\delta^{13}\text{C}$ changes observed and also by the good synchronicity between $\delta^{13}\text{C}$ and $\delta^{18}\text{O}$ records. This can be explained by a relatively good preservation of the soils during cold periods permitting a fast start to re-vegetation. A record from Monticchio lake has shown a similarly rapid reaction of vegetation to rapid temperature changes¹³. On the contrary, a significant time delay of 1–2 kyr seems to have occurred after the ‘Villars cold phase’,

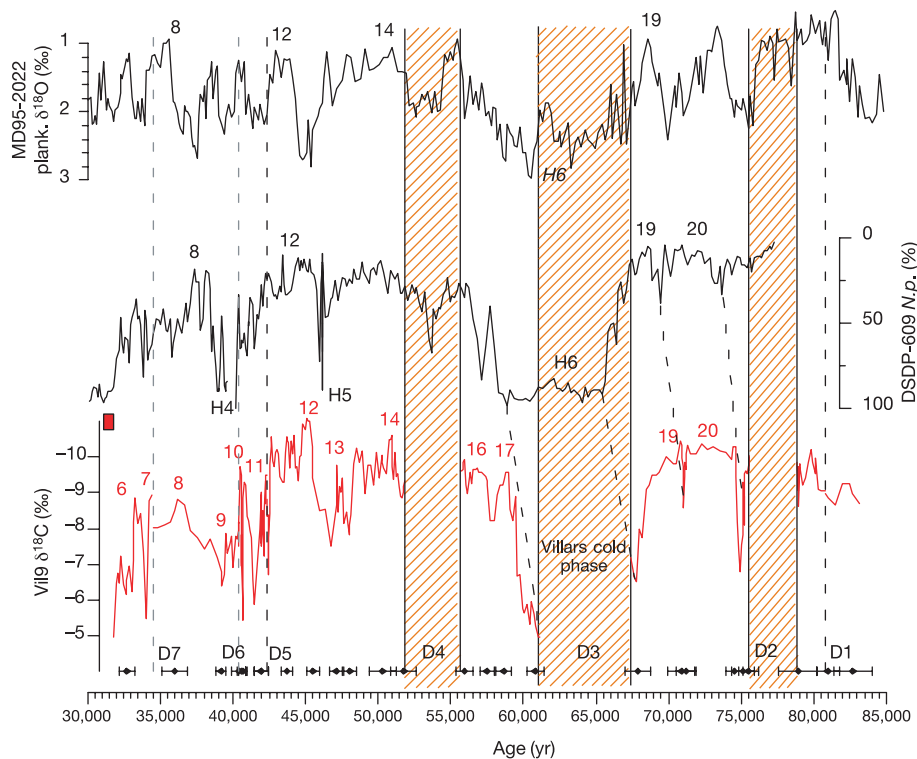


Figure 3 Vil9 $\delta^{13}\text{C}$ record compared with the percentage of *Neoglobigerina pachyderma* of the marine core DSDP 6095, and with planktonic foraminifera $\delta^{18}\text{O}$ of core MD95-2042 (southwest Portugal)⁶. Shape similarities between Vil9 and DSDP 609 records are particularly striking for the oldest part of the record (>50 kyr ago), highlighting the occurrence of a long cold period between 61.2 ± 0.59 and

67.4 ± 0.87 kyr ago that we called the ‘Villars cold phase’. It suggests that the local temperature was very similar to the regional SST, imprinted in the marine core records, and followed the warming–cooling events. Coloured vertical bars represent growth hiatuses.

as shown by the long and regular $\delta^{13}\text{C}$ decrease demonstrating the harshness of this period (Fig. 2). Finally, temperature variation might also have played a significant role in the $\delta^{13}\text{C}$ changes: equilibrium fractionation during soil CO_2 dissolution and during calcite precipitation in the cave, leading to an average $\delta^{13}\text{C}$ gradient of -0.1‰ per $^\circ\text{C}$ (ref. 21), might explain about 20% of the observed $\delta^{13}\text{C}$ variations.

On the Vil9 stalagmite, the sequence of DO events is less clearly depicted in the $\delta^{18}\text{O}$ than in the $\delta^{13}\text{C}$ record (Fig. 4). In addition to the well-marked DO 12 event, the $\delta^{18}\text{O}$ record shows significant general increasing trends between 75.5 and 67.4 kyr ago ($+2.1\text{‰}$) and between 51.8 to 31.8 kyr ago ($+1.4\text{‰}$). Those trends parallel the SPECMAP and the benthic MD-95-2042 records, leading to the hypothesis that they result from the deterioration of the global climate. Superimposed on these general features, the Vil9 $\delta^{18}\text{O}$ record shows changes associated with DO events probably linked with the temperature changes (Fig. 4).

An estimation of the temperature (Fig. 4) shows a drop between 75 and 67.4 kyr ago of $-13.6 \pm 2^\circ\text{C}$, which, compared to the present-day temperature ($12.5 \pm 0.5^\circ\text{C}$), suggests that the local temperature was close to freezing just before the 6.2-kyr-long

'Villars cold phase'. This period fits well with the GRIP ss09 record where ice $\delta^{18}\text{O}$ stayed generally low (-42‰), and was punctuated by two warming events (DO 18 and another one) that were too short to start the seepage water process again above the Villars cave. We suppose that during this non-deposition period (D3) a permafrost occurred above the Villars cave. The stalagmite stopped growing after a general cooling trend punctuated by nine DO events and marked, at the end, by the lowest growth rate (0.01 mm yr^{-1} between 38.9 and 31.9 kyr ago). During this last cooling trend, DO 12 is the most pronounced event, characterized by the highest growth rate and the highest $\delta^{18}\text{O}$ variation ($>1.2\text{‰}$) between the coldest and the warmest phase. Applying the same assumptions as for the 75.5–67.4 kyr trend period implies a temperature increase of more than 10°C , which is in good agreement with marine cores¹¹ ($\sim 10^\circ\text{C}$) and pollen records from lakes in southern and eastern France¹² ($\sim 8^\circ\text{C}$).

Southwest France (and more generally, southwest Europe) possesses many caves that, given their southern location away from the British Isles, Ireland and Fennoscandian ice sheets, surely recorded DO events in the same way as the Vil9 stalagmite. The wide availability of TIMS uranium dates permits precise chronologies

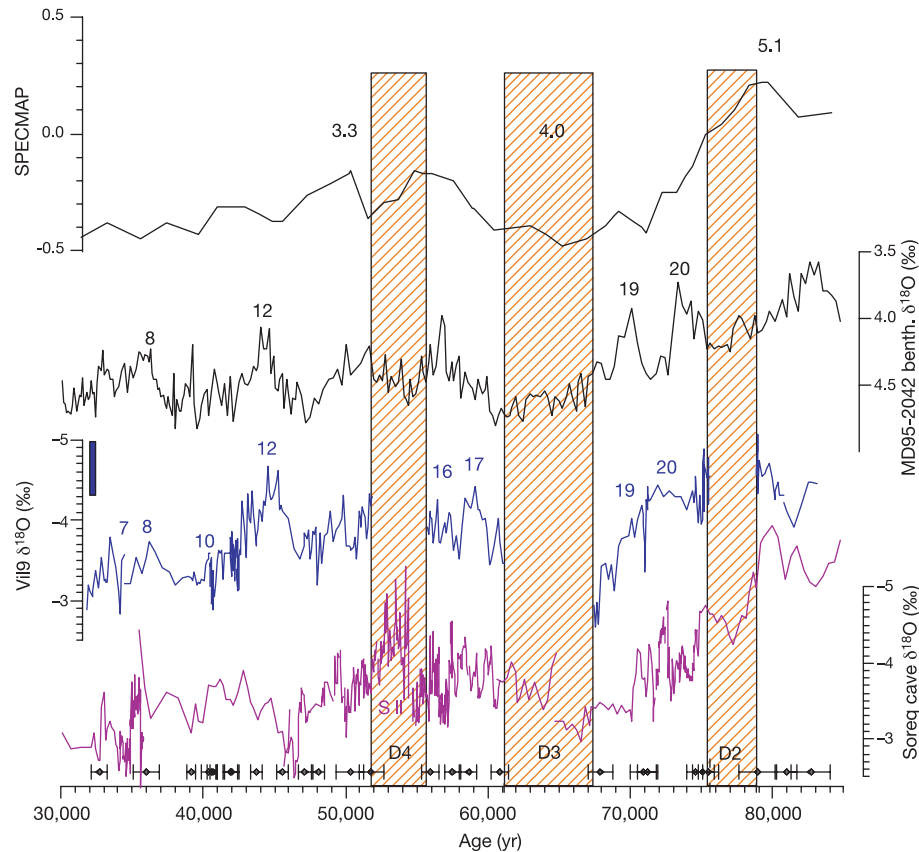


Figure 4 Comparison of the Vil9 $\delta^{18}\text{O}$ record with the Soreq cave $\delta^{18}\text{O}$ record⁴, benthic foraminifera $\delta^{18}\text{O}$ of marine core MD95-2042⁶, and SPECMAP $\delta^{18}\text{O}$ normalized record with MIS numbers. Modern calcite $\delta^{18}\text{O}$ values at Villars are shown by the rectangle on the left. There is a marked resemblance between Vil9 and Soreq cave $\delta^{18}\text{O}$ records, not only in the general trends but also in the absolute $\delta^{18}\text{O}$ values. This suggests that both records are affected in a similar way by the general climate deterioration associated with the growth of continental ice sheets. Small differences, for example the absence of the DO 12 event in the Soreq record, or the absence of Sapropel 2 in Villars record (D4), are the consequences of climate regional influences and/or local geomorphology factors which allow or prevent flooding in the cave. As pointed out by many authors^{4,18,19,27}, the speleothem $\delta^{18}\text{O}$ signal is influenced by many parameters: the seepage water $\delta^{18}\text{O}$ ($\delta^{18}\text{O}_w$), the ocean $\delta^{18}\text{O}$, the depression path, the local temperature, the seasonality of the

precipitation and finally the calcite deposition conditions (temperature, isotopic equilibrium), where temperature-dependent fractionation during calcite precipitation acts in the opposite way to external temperature (about -0.23‰ per $^\circ\text{C}$; ref. 28). Theoretically, calculation of past temperatures is possible if $\delta^{18}\text{O}_w$ can be estimated or, better, deduced from fluid inclusions trapped in the calcite lattice²⁹. Measurements of fluid inclusions are under development in our laboratory; here we tentatively follow the first approach in assuming that the change of $\delta^{18}\text{O}_w$ for the coldest period (67.4 kyr ago) with respect to its present-day value is close to the change estimated for the last glacial over western Europe ($-1.5 \pm 0.5\text{‰}$; ref. 30), and that during the warmest phase of this period, at 75 kyr ago, $\delta^{18}\text{O}_w$ was close to its present-day value (average seepage water $\delta^{18}\text{O}$ measured in Villars cave is $-6.3 \pm 0.1\text{‰}$).

for climate events to be developed for the past 400 kyr. This constrains not only ice-core chronologies, but also all other records that are dependent upon ice-core timescales. For example, a simple intercomparison between VIL9 and GRIP records permits the precise dating of the late glacial ¹⁰Be peak, which largely covers DO 10 (ref. 22), an event extending between 40.4 and 41.5 kyr ago in the VIL9 record. Finally, it is likely that such large climatic oscillations have affected past human cultures, causing migrations and changes in living and eating habits. Archaeological remains, which can be time constrained thanks to calcite deposits found in prehistoric shelters, can then be put in a climatic framework that will lead to a better understanding of these past cultures²³. □

Received 27 September; accepted 23 December 2002; doi:10.1038/nature01391.

1. Labeyrie, L. Glacial climate instability. *Science* **290**, 1905–1907 (2000).
2. Blunier, Th. & Brook, E. J. Timing of millennial-scale climate change in Antarctica and Greenland during the last glacial period. *Science* **291**, 109–112 (2001).
3. Bond, G. C. *et al.* Persistent solar influence on North Atlantic climate during the Holocene. *Science* **294**, 2130–2136 (2001).
4. Bar-Matthews, M., Ayalon, A. & Kaufmann, A. Timing and hydrological conditions of sapropel events in the Eastern Mediterranean, as evidence from speleothems, Soreq Cave. *Chem. Geol.* **169**, 145–156 (2000).
5. Bond, G. *et al.* Correlations between climate records from North Atlantic sediment and Greenland ice. *Nature* **365**, 143–147 (1993).
6. Shackleton, N. J. & Hall, M. A. Phase relationships between millennial-scale events 64,000–24,000 years ago. *Paleoceanography* **15**, 565–569 (2001).
7. Johnsen, S. J. *et al.* Irregular glacial interstadials recorded in a new Greenland ice core. *Nature* **359**, 311–313 (1992).
8. Dansgaard, W. *et al.* Evidence for general instability of past climate from a 250-kyr ice-core record. *Nature* **364**, 218–220 (1993).
9. Grootes, P. M., Stuiver, M., White, J. W. C., Johnsen, S. J. & Jouzel, J. Comparison of the oxygen isotope records from the GISP2 and GRIP Greenland ice cores. *Nature* **366**, 552–554 (1993).
10. Cacho, I. *et al.* Dansgaard-Oeschger and Heinrich event imprints in Alboran Sea paleotemperatures. *Paleoceanography* **14**, 698–705 (1999).
11. Cayre, O., Lancelot, Y., Vincent, E. & Hall, M. A. Paleoclimatological reconstructions from planktonic foraminifera of the Iberian margin: Temperature, salinity, and Heinrich events. *Paleoceanography* **14**, 384–396 (1999).
12. Guiot, J. *et al.* The climate in Western Europe during the last glacial/interglacial cycle derived from pollen and insect remains. *Palaeogeogr. Palaeoclimatol. Palaeoecol.* **103**, 73–93 (1993).
13. Allen, J. R. M. *et al.* Rapid environmental changes in southern Europe during the last glacial period. *Nature* **400**, 740–743 (1999).
14. Bender, M. *et al.* Climate connection between Greenland and Antarctica during the last 100,000 years. *Nature* **372**, 663–666 (1994).
15. Lang, C. *et al.* 16°C rapid temperature variation in Central Greenland 70000 years ago. *Science* **286**, 934–937 (1999).
16. Beck, W. J. *et al.* Extremely large variations of atmospheric ¹⁴C concentration during the last glacial period. *Science* **292**, 2453–2458 (2001).
17. Genty, D. *et al.* Dead carbon in stalagmites: limestone paleodissolution versus ageing of soil organic matter—Implications for ¹³C variations in stalagmites. *Geochim. Cosmochim. Acta* **65**, 3443–3457 (2001).
18. Wang, Y. J. *et al.* A high-resolution absolute-dated late Pleistocene monsoon record from Hulu Cave, China. *Science* **294**, 2345–2348 (2001).
19. Doralé, J. A., Edwards, R. L., Ito, E. & Gonzalez, L. Climate and vegetation history of the midcontinent from 75 to 24 ka: A speleothem record from Crevice Cave, Missouri, USA. *Science* **282**, 1871–1874 (1998).
20. Urbanc, J., Pezdic, J., Dolenc, T. & Perko, S. Isotopic composition of oxygen and carbon in cave water and speleothems of Slovenia. *Acta Carsologica* **13**(4), 99–112 (1985) (in Slovenian).
21. Mook, W. G. in *Handbook of Environmental Geochemistry* (eds Fritz, P. & Fontes, J. Ch.) Vol. 1-A, 49–74 (Elsevier Science, Amsterdam, 1980).
22. Yiou, F. *et al.* Beryllium 10 in the Greenland Ice Core Project ice core at Summit Greenland. *J. Geophys. Res.* **102**, 26783–26794 (1997).
23. Stringer, C. & Davies, W. Those elusive Neanderthals. *Nature* **413**, 791–792 (2001).
24. Johnsen, S. J. *et al.* Oxygen isotope and paleotemperature records from six Greenland ice-core stations: Camp Century, Dye-3, GRIP, GISP2, Renland and North GRIP. *J. Quat. Sci.* **16**, 299–307 (2001).
25. Baker, A., Smart, P. L., Edwards, R. L. & Richards, D. A. Annual growth bandings in a cave stalagmite. *Nature* **364**, 518–520 (1993).
26. Genty, D. & Quinif, Y. Annually laminated sequences in the internal structure of some Belgian stalagmites—Importance for paleoclimatology. *J. Sedim. Res.* **66**, 275–288 (1996).
27. Hendy, C. H. The isotopic geochemistry of speleothems—I. The calculation of the effects of different modes of formation on the isotopic composition of speleothems and their applicability as paleoclimatic indicators. *Geochim. Cosmochim. Acta* **35**, 801–824 (1971).
28. O’Neil, J. R., Clayton, R. N. & Mayeda, T. K. Oxygen isotope fractionation in divalent metal carbonates. *J. Chem. Phys.* **51**, 5547–5558 (1969).
29. Dennis, P. F., Rowe, P. J. & Atkinson, T. C. The recovery and isotopic measurement of water from fluid inclusions in speleothems. *Geochim. Cosmochim. Acta* **65**, 871–884 (2001).
30. Rozanski, K. Deuterium and oxygen-18 in European groundwaters—Links to atmospheric circulation in the past. *Chem. Geol.* **52**, 349–363 (1985).

Supplementary Information accompanies the paper on Nature’s website (http://www.nature.com/nature).

Acknowledgements We thank H. Versaveau and Th. Baritaud for help in sampling, and C. Waelbroeck, U. von Grafenstein, G. Hoffmann, D. Joly and M. F. Diot for discussions. This work was supported by NERC, CNRS–INSU (VariEnTe, Eclipse, PNEDC) and the CEA.

Competing interests statement The authors declare that they have no competing financial interests.

Correspondence and requests for materials should be addressed to D.G. (e-mail: genty@lsce.saclay.cea.fr).

New ages for human occupation and climatic change at Lake Mungo, Australia

James M. Bowler*†, Harvey Johnston‡, Jon M. Olley§, John R. Prescott||, Richard G. Roberts†¶, Wilfred Shawcross# & Nigel A. Spooner*†☆☆

* School of Earth Sciences, University of Melbourne, Melbourne, Victoria 3010, Australia
 † NSW National Parks & Wildlife Service, Buronga, New South Wales 2739, Australia
 § CSIRO Land & Water, Canberra, Australian Capital Territory 2601, Australia
 || Department of Physics & Mathematical Physics, University of Adelaide, Adelaide, South Australia 5005, Australia
 ¶ School of Geosciences, University of Wollongong, Wollongong, New South Wales 2522, Australia
 # 25 Fairfax Street, O’Connor, Canberra, Australian Capital Territory 2602, Australia
 ☆ Research School of Earth Sciences, Australian National University, Canberra, Australian Capital Territory 0200, Australia
 ‡ These authors contributed equally to this work

Australia’s oldest human remains, found at Lake Mungo, include the world’s oldest ritual ochre burial (Mungo III)¹ and the first recorded cremation (Mungo I)². Until now, the importance of these finds has been constrained by limited chronologies and palaeoenvironmental information³. Mungo III, the source of the world’s oldest human mitochondrial DNA⁴, has been variously estimated at 30 thousand years (kyr) old¹, 42–45 kyr old^{5,6} and 62 ± 6 kyr old^{7,8}, while radiocarbon estimates placed the Mungo I cremation near 20–26 kyr ago^{2,9,10}. Here we report a new series of 25 optical ages showing that both burials occurred at 40 ± 2 kyr ago and that humans were present at Lake Mungo by 50–46 kyr ago, synchronously with, or soon after, initial occupation of northern^{11,12} and western Australia¹³. Stratigraphic evidence indicates fluctuations between lake-full and drier conditions from 50 to 40 kyr ago, simultaneously with increased dust deposition, human arrival and continent-wide extinction of the megafauna^{14,15}. This was followed by sustained aridity between 40 and 30 kyr ago. This new chronology corrects previous estimates for human burials at this important site and provides a new picture of *Homo sapiens* adapting to deteriorating climate in the world’s driest inhabited continent.

Lake Mungo, the centrepiece of the Willandra Lakes World Heritage Area in western New South Wales, boasts several features of significance to world archaeology, such as Quaternary climate change and the interaction of early humans with the Australian landscape and biota. It is also the type site for the Lake Mungo Geomagnetic Excursion¹⁶.

Fed by an ancestral course of the Lachlan River rising in the highland catchments near Canberra (Fig. 1), the hydrologic record from the now dry lake basin reflects Pleistocene changes in

** Present address: DSTO, Edinburgh, South Australia 5111, Australia.